How Simulations of the Land Carbon Sink Are Biased by Ignoring Fluvial Carbon Transfers: A Case Study for the Amazon Basin

Ronny Lauerwald, Pierre Régnier, Bertrand Guenet, Pierre Friedlingstein, Philippe Ciais

One Earth

Article

How Simulations of the Land Carbon Sink Are Biased by Ignoring Fluvial Carbon Transfers: A Case Study for the Amazon Basin

Graphical Abstract

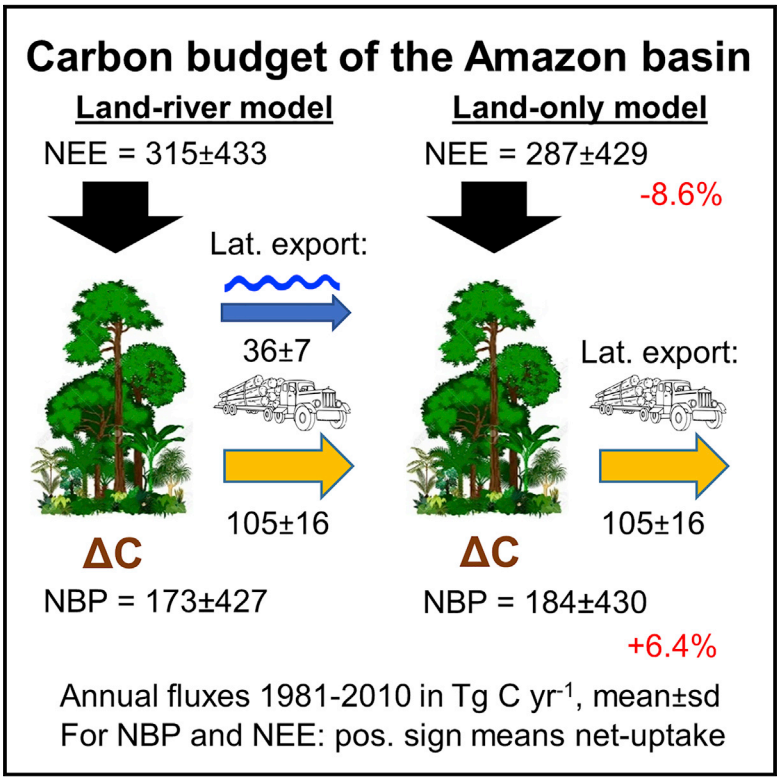

Highlights

- Ignoring fluvial C exports leads to underestimation of the land uptake of CO_2
- Ignoring fluvial C exports leads to overestimation of land C stock increases
- Biases scale to fluvial C exports to the coast rather than to aquatic CO_2 emissions
- Future fluvial C exports are likely to increase with runoff and primary production

Authors

Ronny Lauerwald, Pierre Regnier, Bertrand Guenet, Pierre Friedlingstein, Philippe Ciais

Correspondence

ronny.lauerwal@gmail.com

In Brief

In nature, carbon fixed by land ecosystems is either stored in biomass and soils or leached to rivers where it is decomposed or transferred to the ocean. In carbon cycle models, this river loop of the carbon cycle is ignored. Using a novel model of the coupled land-river carbon cycle and the Amazon basin as a test case, we show that ignoring the river carbon loop leads to significant biases in the simulation of the land carbon budget.

Lauerwald et al., 2020, One Earth *3*, 226–236
August 21, 2020
https://doi.org/10.1016/j.oneear.2020.07.009

CellPress

CellPress OPEN ACCESS
Gold Standard for the Global Goals
3 tons of CO_2 offset

One Earth

Article

How Simulations of the Land Carbon Sink Are Biased by Ignoring Fluvial Carbon Transfers: A Case Study for the Amazon Basin

Ronny Lauerwald,[1,2,3,7,*] Pierre Regnier,[2] Bertrand Guenet,[1,4] Pierre Friedlingstein,[5,6] and Philippe Ciais[1]
[1]Laboratoire des Sciences du Climat et de l'Environnement, IPSL, CEA Saclay, Bat 714, Site de l'Orme des Merisiers, Chemin de Saint Aubin - RD 128, Gif-sur-Yvette 91191, France
[2]Biogeochemistry and Earth System Modelling, Department of Geoscience, Environment and Society, Université Libre de Bruxelles, CP 160/02, 50, avenue F.D. Roosevelt, Brussels 1050, Belgium
[3]Université Paris-Saclay, INRAE, AgroParisTech, UMR ECOSYS, Thiverval-Grignon 78850, France
[4]Laboratoire de Géologie, École Normale Supérieure/CNRS UMR8538, PSL Research University, 24 Rue Lhomond, Paris 75005, France
[5]Mathematical Modelling of Climate Systems, CEMPS, University of Exeter, Laver Building, Exeter EX4 4QE, UK
[6]LMD/IPSL, ENS, PSL Université, École Polytechnique, Institut Polytechnique de Paris, Sorbonne Université, CNRS, Paris, France
[7]Lead Contact
*Correspondence: ronny.lauerwal@gmail.com
https://doi.org/10.1016/j.oneear.2020.07.009

SCIENCE FOR SOCIETY Terrestrial ecosystems absorb, at present, about one-fourth of anthropogenic CO_2 emissions, which is accumulating in the carbon (C) stocks of vegetation and soils. Land-surface models are used to project the 21st century evolution of this CO_2 sink, which mitigates the expected increase in atmospheric CO_2 concentration and, thus, climate change. However, classical land-surface models neglect that a fraction of the anthropogenic C absorbed by terrestrial ecosystems is not accumulating on land but is instead exported through the river network. Using the Amazon basin as a case study and a novel land-surface model that represents C exports through rivers, we prove that classical land-surface models such as those used for the Assessment Reports of the IPCC underestimate the CO_2 uptake by terrestrial ecosystems and overestimate the amount of anthropogenic C sequestered within vegetation and soils. We provide reasons justifying that similar biases are to be expected at global scale.

SUMMARY

Land-surface models are important tools for simulation of the past, present, and future capacity of terrestrial ecosystems to absorb anthropogenic CO_2 emissions. However, fluvial carbon (C) transfers are presently neglected in these models. Using the Amazon basin as a case study, we show that this negligence leads to significant underestimation of the net uptake of atmospheric C while terrestrial C storage changes are overestimated. These biases arise from the fact that C—in reality, leached from soils and exported through the river network—is instead represented as partly being respired and partly being stored in soils. Moreover, these biases scale mainly to the fluvial C export to the coast, despite aquatic CO_2 emission to the atmosphere being the major pathway of riverine C exports. We further show that fluvial C transfers may change significantly in response to changes in either hydrology or in atmospheric C uptake by vegetation.

INTRODUCTION

The inland water network plays an important role in the global carbon (C) cycle, as a major transfer route of land-derived C to the ocean as well as an efficient biogeochemical reactor where large amounts of terrestrial organic C inputs are processed, feeding a net CO_2 evasion that is larger than the exports of C to the coast.[1] In quantitative terms, both the total inputs of C from terrestrial ecosystem into inland waters and the CO_2 evasion from inland waters remain largely uncertain at global scale, as demonstrated by different estimates published over the last decade (see review by Drake et al.[2]). Moreover, a recent study has demonstrated that even fluvial C exports to the coast, although long assumed to be rather well constrained, are likely underestimated.[3] While the C inputs from soils to inland waters (1.1–5.1 Pg C $year^{-1}$)[2] are relatively small compared with terrestrial net primary production (NPP), they are comparable in magnitude with the global change in forest C storage of 2.4 ± 0.4 Pg C $year^{-1}$[4] averaged over the

1990–2007 period. Given that global change affects the land C budgets and terrestrial C exports through the inland water network simultaneously,[5] it is necessary to assess their temporal evolution at the same time.

Earth system models (ESMs), which are used to simulate the coupled evolution of the C cycle and the climate system in response to anthropogenic CO_2 emissions and land-use change, do not represent inland waters as transport routes of C from land to ocean nor as CO_2 source to the atmosphere. However, over the last couple of years a number of specialized branches of land-surface models have been developed to represent fluvial transfers of C,[6–8] which could in theory be used as land-surface schemes in an ESM framework. The use of those models has so far, however, been limited to regional scale applications. Other land-surface models have been enabled to represent the leaching of dissolved organic C (DOC) from soils, though not its lateral transfer through river catchments or its fate in the inland water network.[9,10] None of these studies explored the role of fluvial C transfers on the terrestrial C budget. Most importantly, it remains unknown how the omission of fluvial C transfers in classical land-surface models affects the simulation of the land C sink. Given the magnitude of fluvial C transfers, the main hypothesis of this study is that this bias is substantial.

The recently developed model ORCHILEAK, a new branch of the Institut Pierre Simon Laplace (IPSL) ESM land-surface scheme ORCHIDEE (Organizing Carbon and Hydrology In Dynamic Ecosystems), simulates vegetation and soil C processes as well as DOC and CO_2 transport along the terrestrial-aquatic continuum of the Amazon basin, and was found to reproduce observed spatiotemporal patterns sufficiently well for present-day conditions[11,12] (see Lauerwald et al.[11] for a detailed model description and evaluation against observational data, which include NPP for evergreen and rain-green tropical forest, C3 and C4 grassland and C4 cropland as major vegetation types, magnitude and temporal variability of discharge and DOC fluxes in the Amazon river and its major tributaries, seasonality in floodplain inundation, and aquatic CO_2 emission from the river-floodplain network). The Amazon basin has been a subject of research for many years because of its high potential as a C sink to mitigate increasing atmospheric CO_2 and the coincident negative impacts of land-use change and climate change on C storage.[13–16] The Amazon is a hotspot of the inland water C cycle because of the large leaching rates of dissolved organic carbon (DOC) from soils and productive vegetation, the very high CO_2 emission rates from surface waters, and the substantial contribution of floodplains in the overall C balance.[17–19] The exports of terrestrially derived C through the Amazon river network are substantially higher than the fossil fuel emissions of the whole of South America,[20] and should thus not be ignored in regional C budgets. The Amazon basin is thus the optimal test case for exploration of the role of fluvial C transfers in the land C budget and assessment of the bias that is made when simulating the land C sink with a classical land-surface model ignoring these fluvial C transfers.

In 2002, Richey et al.[17] revealed the large magnitude of aquatic CO_2 emissions from the river-floodplain network of the Amazon basin, calling for the inclusion of those fluxes into the C budget of the Amazon rain forest. The authors assumed that the aquatic CO_2 emissions is mainly fueled by in-stream respiration of organic C inputs from *terra firme* ecosystems and floodplains,[17] which means that in the long run, aquatic CO_2 emission would represent a fraction of NPP. A more recent study[21] has shown, however, that the integration of these emissions into the basin-wide C budget is more complex, in particular because a part of the CO_2 in the river comes from respiration in *terra firme* and floodplain soils, of which in turn a part is contributed by autotrophic root respiration rather than heterotrophic respiration in the river. The second main hypothesis followed in this study is thus that aquatic CO_2 emission and fluvial C exports to the coast should be compared with the gross primary production (GPP) rather than with NPP. ORCHILEAK explicitly represents the various sources of organic C and CO_2 to the river network, including organic matter decomposition and root respiration in *terra firme* soils, inundated floodplain soils, and the water column, and is thus the ideal tool for elucidating the role of aquatic CO_2 emissions and fluvial C transfers in the overall C budget of the Amazon basin.

In this study, we use ORCHILEAK to simulate the coupled evolution of the land C sink and fluvial C transfers in the Amazon basin over the historical period (since 1861) and in the future until the end of the 21st century, following the scenario RCP6.0, which is close to no mitigation. More precisely, we simulate both the net uptake of atmospheric C, i.e., the net ecosystem exchange (NEE), and the change in terrestrial C storage, i.e., the net biome production (NBP), explicitly accounting for the C transfers through the river-floodplain network. To quantify the bias associated with the use of classical land-surface models that are not representing fluvial C transfers, ORCHILEAK is run in an alternative configuration with fluvial C transfers deactivated.

RESULTS AND DISCUSSION

Present-Day (1981–2010) C Budget of the Amazon Basin

The suitability of a land-surface model to predict changes in NEE and NBP at the centennial timescale depends on its ability to reproduce present-day terrestrial C stocks. In our study, we define the present day as the period 1981–2010, corresponding to the three decades during which most of the observational data used for model validation were collected.[11] In the following, we report simulated fluxes as mean ± standard deviation of annual fluxes over this period. According to our simulation results, the C stored in the terrestrial biomass of the Amazon basin amounts to 91 Pg C, of which 87 Pg C is attributed to tropical rain forest. The simulated aboveground wood biomass (AGB) for the tropical rain forest of 13.0 ± 2.8 kg C m^{-2} is comparable with the average observed AGB of 15.3 kg C m^{-2} in the Amazon basin.[22] The simulated NPP amounts to 6,407 ± 489 Tg C $year^{-1}$, which agrees well with the remotely sensing based estimate for the same area of 6,350 Tg C $year^{-1}$.[23] The simulated soil organic carbon (SOC) stock (excluding litter) amounts to 69 Pg C, of which 48 Pg C is stored in the first meter of the soil profile, i.e., at the higher end of existing data-driven estimates of 41–47 Pg C.[24]

The major innovative aspect of our model approach stems from the inclusion of the river-floodplain network and lateral transfers of C (DOC and CO_2) into the terrestrial C budget. For the present day (1981–2010), we simulate an annual fluvial C export from the Amazon basin to the coast ($F_{w\text{-}c}$) of 36 ± 7 Tg C $year^{-1}$. Of that flux, 29 ± 5 Tg C $year^{-1}$ is in the form of DOC

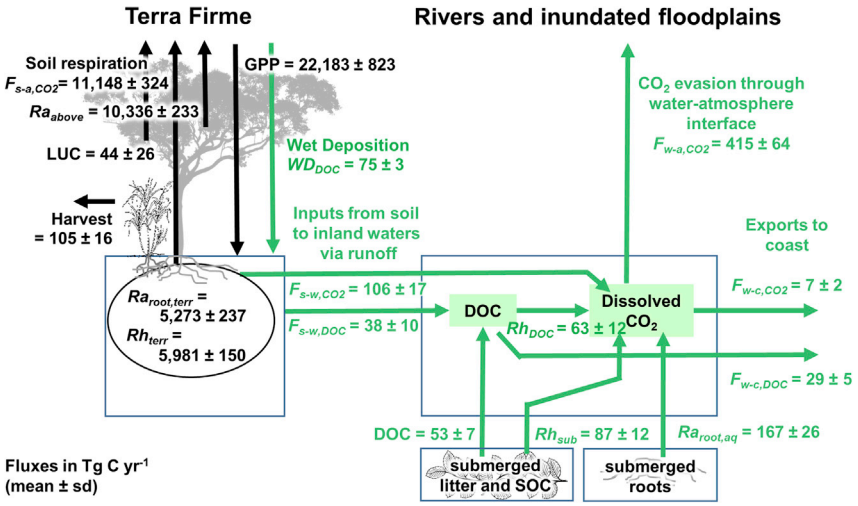

Figure 1. Present-Day C Fluxes through the Terrestrial-Aquatic Continuum of the Amazon Basin Simulated with the "Land-River" Model Configuration

Reported are means and standard deviation of annual fluxes over the period 1981–2010. The C fluxes in ORCHILEAK usually not represented in land-surface models are highlighted in green. See Table 1 for definition of abbreviations.

(Figure 1; for abbreviations see Table 1) and the rest is dissolved CO_2. While we represent the Amazon river down to its mouth at Macapá, the furthest downstream location for which fluvial DOC fluxes are reported is Óbidos, about 900 km upstream from the mouth. If we take the observation-based estimate of a fluvial DOC flux of 27 Tg C $year^{-1}$ at Óbidos for the period 1994–2000,[18] scale this flux to the increase in discharge down to Macapá (see Experimental Procedures), and apply the observation that DOC concentrations increase about 10% over this river stretch,[25] we estimate a fluvial DOC export from the Amazon basin of 33 Tg C $year^{-1}$, which is close to our simulation result.

Lateral export flux of dissolved CO_2 is not explicitly reported in the literature. Instead, fluvial fluxes of dissolved inorganic carbon (DIC) are typically reported,[30] which are dominated by bicarbonate ions counterbalanced by base cations (carbonate alkalinity) mobilized in the process of chemical rock weathering. Note that these processes are not represented in ORCHILEAK, and it is thus not possible to reproduce the observed exports of total DIC. However, we can calculate an estimate of fluvial export of free dissolved CO_2 using the values of CO_2 partial pressures reported at Macapá.[31] Assuming a water temperature of 29°C (average water temperature in lower mainstem; see Lauerwald et al.[11]) to convert those values to CO_2 concentrations, and multiplying by the average discharge from the Amazon of 197,426 m^3 s^{-1} (see Experimental Procedures), we calculate an observation-based fluvial CO_2 export $F_{w\text{-}c,CO2}$ of 7 Tg C $year^{-1}$, which is comparable with our simulation result of 7 ± 2 Tg C $year^{-1}$. Furthermore, while we represent the local decomposition of submerged plant litter and soil organic C in the inland water network as an additional source of DOC and CO_2 to the water column (see Lauerwald et al.[11]), we neglect transport of particulate organic C. This is, however, of minor importance for the C budget of the Amazon basin, as the particulate fraction of the fluvial organic C load amounts to only about 10% at the basin outlet.[25] The simulated CO_2 evasion from the inland water network $F_{w\text{-}a,CO2}$ (river and inundated floodplains) amounts to 415 ± 64 Tg C $year^{-1}$, which is comparable with the observation-based estimate of 470 Tg C $year^{-1}$ by Richey et al.[17] The simulated CO_2 evasion from the water surface is thus about one order of magnitude higher than the lateral C export to the coast, in agreement with field studies.[17] We thus find that, in addition to the terrestrial C fluxes, our model reproduces the inland water C fluxes reasonably well.

As mentioned earlier, our model offers the possibility to quantitatively attribute $F_{w\text{-}a,CO2}$ to its various sources and to integrate $F_{w\text{-}a,CO2}$ consistently into the C budget of the Amazon basin. To begin with, $F_{w\text{-}a,CO2}$ is about 27 times lower than the simulated CO_2 emissions from soils ($F_{s\text{-}a,CO2}$, Figure 1). This is largely due to the smaller areal proportion of surface waters compared with the one occupied by terrestrial ecosystems. However, even when normalized by area, simulated CO_2 emission rates from rivers and inundated floodplains of 1,511 ± 117 g C m^{-2} $year^{-1}$ are still somewhat lower than the average rates of *terra firme* soil respiration of 1,900 ± 55 g C m^{-2} $year^{-1}$. These modeled rates agree well with observed CO_2 evasion rates from inland waters[32] and with CO_2 emissions from soil respiration studies[33,34] in the Amazon basin. The *terra firme* ecosystems in our simulation act as an overall sink for atmospheric CO_2 because the terrestrial GPP exceeds the sum of $F_{s\text{-}a,CO2}$ and autotrophic respiration of the aboveground plant parts (Ra_{above}). Note that CO_2 emission flux from soils is to a large part sustained by the autotrophic respiration of roots (Ra_{root}) and not by heterotrophic microbial respiration (Rh_{terr}). Across the Amazon basin, Ra_{root} and Rh_{terr} contribute 47% ± 1% and 53% ± 1% of the total soil respiration, respectively (Figure 1), which is in agreement with the previously reported observed range of 42%–61% contribution of Ra_{root} to $F_{s\text{-}a,CO2}$.[35,36]

Inland waters, on the contrary, act mostly as net source of CO_2 fueled by allochthonous C inputs originating from DOC and CO_2 leached from soils.[21] While CO_2 inputs from soil respiration to the river network via runoff ($F_{s\text{-}w,CO2}$) represent only about 1% of total soil respiration, in agreement with data-driven estimates,[37] it contributes one-quarter (25% ± 1% or 106 ± 17 Tg C $year^{-1}$) of the total CO_2 loss from the river-floodplain network, i.e., the sum of $F_{w\text{-}a,CO2}$ and $F_{w\text{-}c,CO2}$ in Figure 1. Therefore, Ra_{root} is a substantial source not only to $F_{s\text{-}a,CO2}$, but also to $F_{s\text{-}w,CO2}$. Also within the river-floodplain network, the simulated respiration of submerged roots ($Ra_{root,aq}$, 167 ± 26 Tg C $year^{-1}$) is of similar magnitude as the heterotrophic respiration of DOC (Rh_{DOC}, 63 ± 13 Tg C $year^{-1}$) and submerged soil carbon and plant litter (Rh_{sub}, 87 ± 12 Tg C $year^{-1}$) ($Rh_{aq} = Rh_{DOC} + Rh_{sub}$ = 150 ± 23 Tg C $year^{-1}$), which contribute to about 40% ± 1% and 36% ± 1% to the total CO_2 exported through the river-floodplain network, respectively. These results highlight the necessity to compare $F_{w\text{-}a,CO2}$ and $F_{w\text{-}c,CO2}$ against GPP instead of NPP, as only half of the CO_2 exports are fed by *Rh*.

Table 1. Definition of Acronyms

Acronym	Definition
DIC	dissolved inorganic C
DOC	dissolved organic C
$F_{s\text{-}a,CO2}$	CO_2 emissions from soil surface
$F_{s\text{-}w,CO2}$	CO_2 inputs to river from *terra firme* soils
$F_{s\text{-}w,DOC}$	DOC inputs to river from *terra firme* soils
$F_{w\text{-}a,CO2}$	CO_2 emissions from water surface
$F_{w\text{-}c,CO2}$	lateral CO_2 export to river mouth
$F_{w\text{-}c,DOC}$	lateral DOC export to river mouth
GPP	gross primary production
Harvest	harvest of crops and wood products
LUC	additional respiration flux due to land-use change
NBP	net biome production
NEE	net ecosystem exchange
NPP	net primary production
POC	particulate organic C
Ra	autotrophic respiration, total
Ra_{above}	*Ra* from aboveground biomass
Ra_{root}	root respiration, total
$Ra_{root,aq}$	root respiration in inundated floodplains
$Rar_{oot,\ terr}$	root respiration in *terra firme* soils
Rh	heterotrophic respiration, total
Rh_{aq}	*Rh* in river network, including inundated floodplains
Rh_{DOC}	*Rh* from decomposition of DOC in water column
Rh_{sub}	*Rh* from decomposition of inundated litter and SOC
Rh_{terr}	*Rh* in and on *Terra Firme* soils
SOC	soil organic carbon
WD_{DOC}	wet deposition (throughfall) of DOC

In our study, we define NEE as the balance between the terrestrial GPP and the wet deposition of DOC (WD_{DOC}) as C inputs from the atmosphere to the Amazon basin and the emissions of CO_2 from *terra firme* soil ($F_{s\text{-}a,CO2}$), aboveground vegetation (Ra_{above}) and water surface ($F_{w\text{-}a,CO2}$) back to the atmosphere (Equation 1 and Figure 1). This equation further includes the on-site respiration of litter resulting from land-use change (LUC). ORCHILEAK does not represent the emission of biogenic volatile organic C (BVOC), which is thus also not included in our calculation of NEE. Note that contrary to the use in other studies,[21] NEE is defined here with the convention of positive sign when C is gained by the land surface and lost by the atmosphere, to be more easily comparable with NBP (see below). For the period 1981–2010, NEE amounts to 315 ± 433 Tg C $year^{-1}$.

The NBP of the Amazon basin is defined as the actual change in C storages of *terra firme* ecosystems and inland waters combined. NBP is here calculated based on the NEE, i.e., the vertical exchanges of C between the atmosphere and the Amazon basin, and the harvest of crops and wood products (*Harvest*) as well as fluvial exports of CO_2 ($F_{w\text{-}c,CO2}$) and DOC ($F_{w\text{-}c,DOC}$) to the coast as lateral export fluxes (Equation 2 and Figure 1). For the present day (1981–2010), the simulated annual NBP in the Amazon basin amounts to 173 ± 427 Tg C $year^{-1}$. For comparison, Gloor et al.[38] estimated an NBP of ~240 ± 298 Tg C $year^{-1}$ for the whole of South America over the period 1980–2009. Our simulated NBP normalized by watershed area equals 29.6 ± 72.8 gC m^{-2} $year^{-1}$ for the present-day period, which is at the low end of the average increase rates of C stocks in American tropical forests estimated by Pan et al.[4] at 77 g C m^{-2} $year^{-1}$ for the period 1990–1999 and 53 g C m^{-2} $year^{-1}$ for the period 2000–2007.

$$\mathrm{NEE} = (\mathrm{GPP} + \mathrm{WD_{DOC}}) - (F_{s\text{-}a,CO2} + Ra_{above} + \mathrm{LUC} + F_{w\text{-}a,CO2})$$

$$= ((22{,}183 \pm 823 + 75 \pm 3) - (11{,}148 \pm 324 + 10{,}336 \pm 233 + 44 \pm 26 + 415 \pm 64))\ \mathrm{Tg\ C\ year^{-1}}$$

$$= 315 \pm 433\ \mathrm{Tg\ C\ year^{-1}}. \qquad \text{(Equation 1)}$$

$$\mathrm{NBP} = \mathrm{NEE} - (F_{w\text{-}c,CO2} + F_{w\text{-}c,DOC} + Harvest)$$

$$= (315 \pm 433 - (7 \pm 2 + 29 \pm 5 + 105 \pm 16))\ \mathrm{Tg\ C\ year^{-1}}$$

$$= 173 \pm 427\ \mathrm{Tg\ C\ year^{-1}} \qquad \text{.(Equation 2)}$$

Equation 2 illustrates how NEE as net uptake of atmospheric C is split into amounts of C accumulating within the Amazon basin (NBP), and lateral exports of C out of the basin related to fluvial transport and the harvest of crop and wood products. Over the period 1981–2010, NBP represents about 55% of the NEE while 11% of NEE is exported to the coast. Note that the fraction of NEE that is accumulating in terrestrial C stocks (NBP) is a consequence of increasing atmospheric CO_2 concentrations, and their fertilizing effect on vegetation and thus represents entirely an anthropogenic perturbation. The same is of course true for harvest and the related export of crops and wood products. In contrast, a certain fraction of C that is channeled through the inland water network would also be exported under steady-state conditions, while the anthropogenic perturbation of this flux remains to be determined (see next section).

While the CO_2 exports from the river-floodplain network ($F_{w\text{-}a,CO2}$ in Figure 1) cannot be regarded as a fraction of the terrestrial NPP within the Amazon basin, the situation is different for fluvial DOC exports, which are mainly sustained by decomposition of litter and SOC. The throughfall flux of DOC ($\mathrm{WD_{DOC}}$), i.e., DOC in the precipitation and DOC washed from the vegetation canopy, is large compared with $F_{w\text{-}c,DOC}$ (Figure 1) and thus needs to be included in a model describing C cycling along the land-river continuum of the Amazon basin. Nevertheless, the major part of $\mathrm{WD_{DOC}}$ infiltrates into the soil where it is respired, while the leaching of DOC from SOC and litter remains the dominant source of DOC to the river. In addition, as we explicitly simulated *Ra* and *Rh* of *terra firme* systems and river-floodplain network (see Figure 1), we can represent NBP also based on the difference between NPP being the major C input flux and total *Rh* being the major output flux (Equation 3). The simulated total annual *Rh* in the Amazon basin amounts to 6,131 ± 165 Tg C $year^{-1}$, of which Rh_{terr} contributes 98% and Rh_{aq} contributes the remaining 2%.

Table 2. Forcing Files Used for Simulations

Variable	Spatial Resolution	Temporal Resolution	Data Source
Rainfall, Snowfall, Incoming shortwave and longwave radiation, Air Temperature, Relative humidity and air pressure (close to surface), Wind speed (10 m above surface)	1°	1 day	ISIMIP2b, IPSL-CM5A-LR model outputs for RCP6.0[26]
Land cover (and change)	0.5°	annual	LUH-CMIP5
Soil texture class	0.5°	–	after HWSD v1.1[27]
Soil pH, bulk density	0.5°	–	after HWSD v1.1[27]
Poor soils	0.5°	–	after HWSD v1.1[27]
Floodplains and swamps	0.5°	–	after Guimberteau et al.[28]
River surface areas (A_{river})	0.5°	–	Lauerwald et al.[29]
Bankfull discharge	1°	–	derived from pre-runs with ORCHILEAK (see text)
95th percentile of water table height over flood plain	1°	–	derived from pre-runs with ORCHILEAK (see text)

$$NBP = (NPP + WD_{DOC}) - (Rh + Harvest + LUC + F_{w\text{-}a,DOC})$$

$$= ((6{,}407 \pm 489 + 75 \pm 3) - (6{,}131 \pm 165 + 105 \pm 16 + 44 \pm 26 + 29 \pm 5))\ Tg\ C\ year^{-1}$$

$$= 173 \pm 427\ Tg\ C\ year^{-1}. \quad \text{(Equation 3)}$$

Effects of Fluvial C Transfers on the Land C Sink

To test the effect of explicitly representing the inland water C cycle on the simulated Amazon C sink, we ran an alternative simulation with the fluvial C-cycle loop being deactivated (Figure 2), which in what follows is termed the "land-only" model in contrast to the "land-river" model presented above. In the land-only model, DOC cycling within the soil column is represented as in the land-river model but without lateral export to the river network. Similarly, CO_2 produced from autotrophic and heterotrophic respiration, including that of litter and SOC decomposition in inundated soils, is entirely feeding into $F_{s\text{-}a,CO2}$. The representation of all other processes and the use of forcing data (Table 2) are exactly the same between the land-river and the land-only model.

Accordingly, GPP, NPP, and total *Ra* are exactly the same in both simulations, although Ra_{root} is not separated into a *terra firme* and a submerged component as in the land-river model. In the land-only model, Rh_{terr} is higher than in the land-river model because DOC and CO_2 are not exported through the river network but released instead by *terra firme* ecosystems. As a result, Rh_{terr} is even slightly higher than the total *Rh* (Rh_{terr} + Rh_{sub} + Rh_{DOC} in Figure 1) simulated with the land-river model, with 6,149 ± 164 Tg C year^{-1} versus 6,131 ± 165 Tg C year^{-1}, respectively.

In the land-only model, NEE and NBP are calculated as follows:

$$NEE = (GPP + WD_{DOC}) - (F_{s\text{-}a,CO2} + Ra_{above} + LUC)$$

$$= ((22{,}183 \pm 823 + 75 \pm 3) - (11{,}589 \pm 363 + 10{,}336 \pm 233 + 44 \pm 26))\ Tg\ C\ year^{-1}$$

$$= 287 \pm 429\ Tg\ C\ year^{-1}. \quad \text{(Equation 4)}$$

$$NBP = NEE - Harvest$$

$$= (287 \pm 429 - 105 \pm 16)\ Tg\ C\ year^{-1}$$

$$= 184 \pm 430\ Tg\ C\ year^{-1} \quad \text{.(Equation 5)}$$

For the present-day period, the NEE simulated by the land-only model (Equation 4) is 27 Tg C year^{-1} (8.6%) lower than in the land-river model (Equation 1). This lower net C uptake from the atmosphere is due to the fluvial C export to the ocean that is not represented in the land-only model, and thus more organic C is respired within the Amazon basin. The non-respired fraction of the fixed C is accumulating in the soil and we find that for the present day, the simulated NBP is 11 Tg C year^{-1} (6.4%) higher in the land-only model (Equation 5) than in the land-river model (Equation 2). Therefore, the difference between both models allows us to elucidate the net effect of the fluvial loop of the C cycle on NEE and NBP.

Temporal Trends at the Centennial Timescale

From the beginning of the industrial period until the present day, we simulate an increase in terrestrial NPP within the Amazon basin by nearly 20% (Figure 3D) following the fertilizing effect of rising atmospheric CO_2 concentrations. That is well within range of the 5%–22% increase in NPP simulated by five different land-surface models taking part in the second Inter-Sectoral Impact Model Intercomparison Project (ISIMIP2) using the same climate forcing data as this study (Figure 4, see Experimental Procedures). *Rh* is largely following this trend, but from the middle of the 20th century, the gap between NPP and *Rh* is increasing (Figure 3D). Accordingly both NEE and NBP increase over the historical period, with a more strongly increasing trend over the last 50 years (Figures 3E–3F). Importantly, the simulated CO_2 evasion ($F_{w\text{-}a,CO2}$) (Figure 3A) from the water surface and lateral DOC ($F_{w\text{-}c,DOC}$) and CO_2 ($F_{w\text{-}c,CO2}$) exports (Figure 3B) from the Amazon basin to the coast do not show a significant trend over the historical period. Moreover, multi-decadal variation of discharge dominates the trends in $F_{w\text{-}c,DOC}$, $F_{w\text{-}a,CO2}$, and $F_{w\text{-}c,CO2}$, and the effects of increasing NPP on the long-term trends in these fluxes are counterbalanced by a decrease of 11% in discharge over the historical period (Figures 3A–3C). Up until the middle of the 20th century, the lateral exports of C to the coast contributed to about 40% of the NEE (Figure 3F). This proportion then started decreasing to about 11% at the present day, due to the increasing contributions of harvesting and NBP (Figures 3E and 3F).

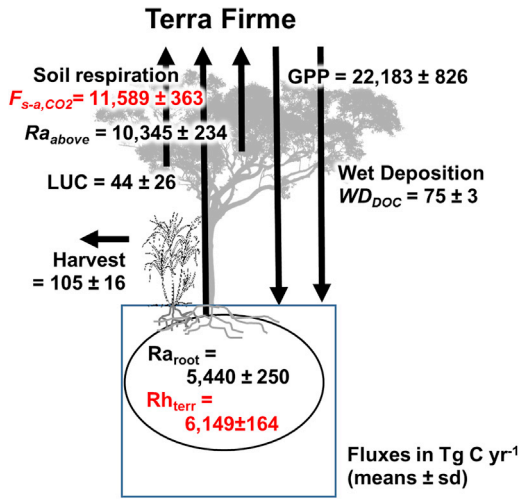

Figure 2. Present-Day C Fluxes in the Amazon Basin Simulated with the "Land-Only" Model Configuration

Reported are means and standard deviation of annual fluxes over the period 1981–2010. The fluxes highlighted in red are also represented in the land-river model, but here reach different values in compensation of the deactivated fluvial C transfers. See Table 1 for definition of abbreviations.

Following the future scenario RCP6.0, which we used here for future projections, terrestrial NPP increases by another 20% over the 21st century. For comparison, the future increase in NPP simulated by five different land-surface models taking part in ISIMIP2 ranges from 16% to 39% (see Experimental Procedures). Note, however, that these future projections are thought to overestimate the CO_2 fertilization effect because important limitations of plant growth are to date ignored in most ESMs, e.g., nutrient limitation (in particular phosphorus)[39] and stand competition.[40] *Rh* follows this trend while the gap between NPP and *Rh* is getting larger (Figure 3D). Both NEE and NBP increase substantially (Figure 3E). Most of the NBP accumulates in the biomass (95%) and only a small amount in the soil C and litter stocks. From the present day (1981–2010) to the end of the 21st century, the biomass increases by an average rate of 0.3% year^{-1}, i.e., similar to the observed average increase rates in aboveground biomass over the last decades of about 0.4% year^{-1}.[14] Contrary to the historical period, there is a substantial increasing trend in the inland water C fluxes (Figures 3A and 3B), following both the accelerated increase in simulated NPP (Figure 3D) but also the trend in discharge that increases again to levels of the early industrial period (Figure 3C). Also, the effect of the multi-decadal variability in discharge on these C fluxes is still visible (Figures 3A–3C). The CO_2 emissions from the river-floodplain network ($F_{w\text{-}a,CO2}$) and fluvial exports of dissolved C to the coast ($F_{w\text{-}c,DOC} + F_{w\text{-}c,CO2}$) increase by 23% and 27%, respectively (Figures 3A and 3B). Nevertheless, the fraction of NEE that is exported to the coast decreases further to about 8% at the end of the 21st century (Figures 3E and 3F).

In steady state, which we assumed for the pre-industrial period, the simulated NBP is zero and NEE is equal to the sum of harvest and fluvial export of C to the coast ($F_{w\text{-}c,CO2} + F_{w\text{-}c,DOC}$) (Figures 3E and 3F). Over the whole simulation period (1861–2099), the C balance of the Amazon basin departs from the steady state due to increasing NPP and the delayed response in *Rh* due to the relatively long residence times of C in biomass and soils (see Bloom et al.[41]). During this period, the net uptake of atmospheric C (NEE) accumulates to 72.1 Pg C, of which 8.9 Pg C (12%) is exported to the ocean ($F_{w\text{-}a,CO2} + F_{w\text{-}c,DOC}$) and 24.1 Pg C (33%) is laterally exported as harvested crops and wood products (*Harvest*, Figures 3D and 3E). The remainder, 39.1 Pg C (54%), represents the NBP that accumulates in the terrestrial C stocks. While *Harvest* and NBP represent or are entirely the consequence of anthropogenic perturbations, only 1.5 Pg C (17%) of the fluvial C exports to the coast are in excess to the simulated pre-industrial values, and are thus assumed to represent the net effect of anthropogenic perturbations on these lateral export fluxes over the simulation period. Looking at the differences in the simulation results with the land-river model versus the land-only model, we find that up to the mid-20th century the net effect of fluvial C transfers on NBP is very low (Figure 3G) because soil and vegetation C stocks are close to steady state and thus NBP is generally low (Figure 3E). The net effect of fluvial C fluxes on the NBP then increases in absolute numbers over the rest of the simulation period, first quite rapidly and then at a rate that is slowing down until the end of the 21st century. At the present day the net effect amounts to 11 Tg C year^{-1}, representing 6.4% of the NBP simulated with the land-river model. At the end of the 21st century the net effect reaches 12 Tg C year^{-1}, but decreases in relative numbers to 4.0% of the NBP simulated with the land-river model. The net effect of fluvial C fluxes on NEE is positive, i.e., more C uptake from the atmosphere is obtained with the land-river model over the whole simulation period. However, NEE shows an interesting long-term trend (Figure 3H): the net effect of fluvial C fluxes on NEE first decreases over the historical period until the late 20th century before it is projected to increase again to a level comparable with that of the late 19th century. This trend is consistent with the difference in *Rh* simulated with the land-river model versus the land-only model (Figure 3I). The decrease over the historical period until the present day is likely due to the stronger accumulation of soil C in the land-river model, which feeds an increasing Rh_{terr}. This effect is then outweighed by the sudden increase in fluvial C exports to the coast over the 21st century (Figure 3B). In relative terms (as percentage of the NEE simulated with the land-river model), the net effect of fluvial C fluxes on simulated NEE decreases over the simulation period from 36% (1861–1890), to 8.6% at the present day, and further down to 5.8% at the end of the 21st century. The difference in NBP simulated by the land-only model relative to that simulated by the land-river model accumulates to 0.6 Pg C (5.1%) and 1.0 Pg C (3.7%) over the periods 1861–2010 and 2011–2099, respectively. For NEE, this difference accumulates to −4.7 Pg C (−20%) and −2.8 Pg C (−5.8%) for the same periods, and to −7.5 Pg C (−10%) over the whole simulation period.

Implications for Global Land C Sink

Our simulations show significant biases in simulated NEE and NBP when fluvial C exports are ignored. These biases are related mainly to lateral exports of C to the coast, while the representation of CO_2 emissions from the river-floodplain network does not significantly affect the C budget of the Amazon basin as a whole. While the Amazon basin is a global hotspot for aquatic CO_2

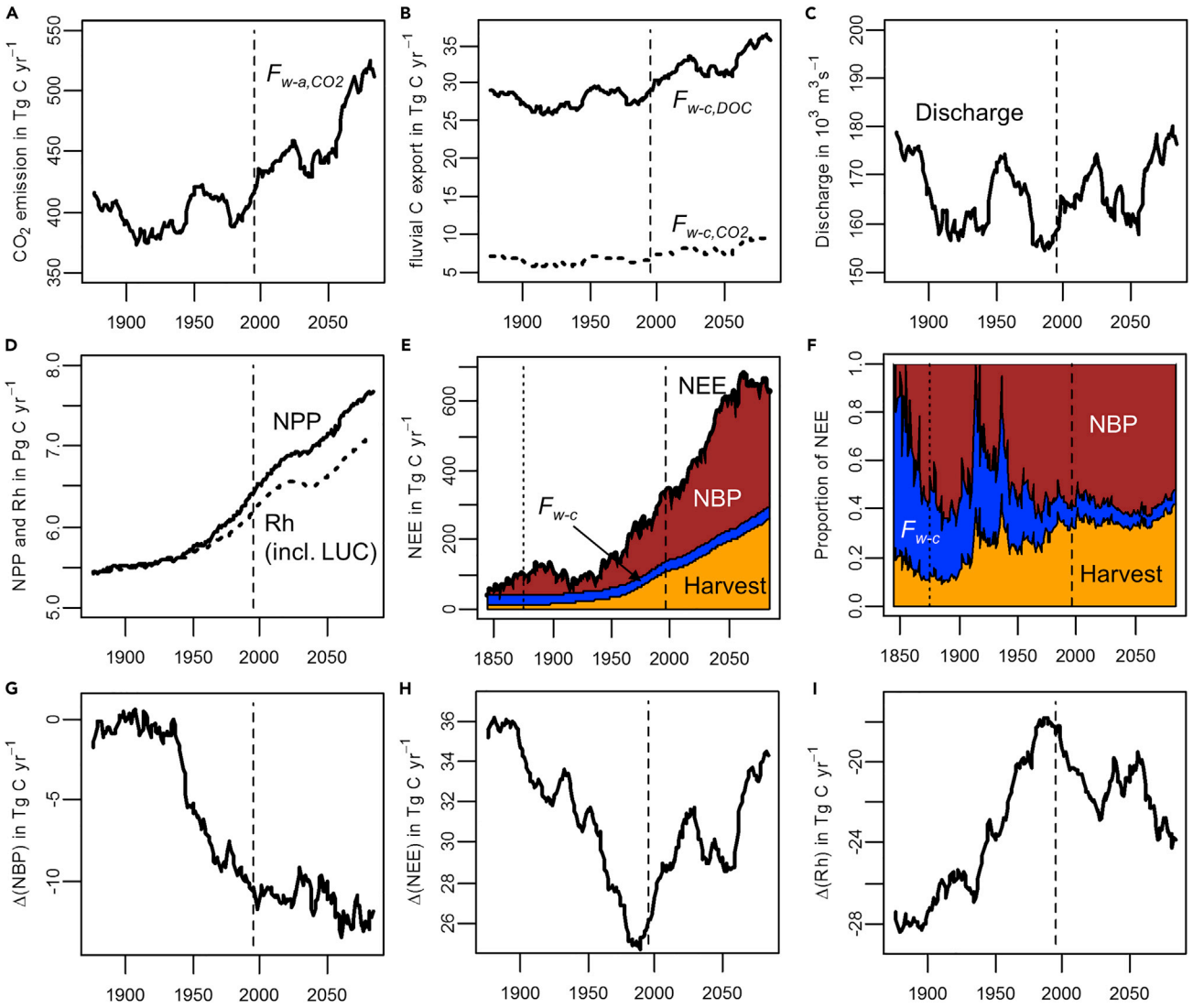

Figure 3. Simulated Long-Term Trends of Hydrology, C Fluxes, and C Budget of the Amazon Basin Obtained with the "Land-River" Model and Co-evolution of the Net Effects of Representing Fluvial C Transfers on the Simulated C Budget

(A–D) The individual panels show temporal trends in (A) CO_2 emissions from the river network to the atmosphere ($F_{w\text{-}a,CO2}$), (B) lateral, fluvial exports of DOC and CO_2 to the coast ($F_{w\text{-}c,DOC}$ and $F_{w\text{-}c,CO2}$, respectively), (C) discharge, and (D) terrestrial net primary production (NPP) and heterotrophic respiration (*Rh*).

(E) Increasing trend in the net C uptake from the atmosphere (NEE), partitioning NEE into the amounts of C removed by harvest (orange shade), exported by rivers to the coast ($F_{w\text{-}c}$, blue shade), and accumulating within the Amazon basin (NBP, brown shade) (compare with Equation 2).

(F) Changes in harvest, $F_{w\text{-}c}$, and NBP relative to NEE over the simulation period (same color code as in E).

(G–I) Net effects of representing fluvial C fluxes on NBP, NEE, and *Rh*, respectively. These effects were calculated by subtracting results of the land-only model from those of the land-river model. All graphs represent 30-year running means of simulation results that suppress interannual variability and reveal temporal trends at the centennial timescale. The dashed vertical line indicates the present day, i.e., the year for which the 30-year running mean corresponds to the average conditions for the period 1981–2010. For both (E) and (F), we added the last 30 years of spin-up before the results of the transient run. Like this, the first 30-year running mean value in these two plots represent the assumed steady state in the pre-industrial period, with an NBP = 0 Tg C $year^{-1}$. The dotted line represents the year 1876, from which the 30-year running mean values are entirely derived from results of the transient simulation runs, consistent with the other plots.

emissions, present-day $F_{w\text{-}c,DOC}$ is not extraordinarily high. According to our simulations, $F_{w\text{-}c,DOC}$ represents only 9.2% of NEE. At global scale, a fluvial DOC export of 200 Tg C $year^{-1}$[42] compared with the average NEE derived from inversions of 2.3 Pg C $year^{-1}$[43] gives a similar ratio of 8.7%. We thus conclude that ignoring fluvial C fluxes leads to similarly important biases at global scale. DOC that should be exported to the coast is instead remaining in the soils, where a part accumulates in the SOC stock (positive bias in NBP) and the remainder is respired *in situ* feeding $F_{s\text{-}a,CO2}$ (negative bias in NEE). It remains nevertheless unclear whether in other climate zones a stronger bias in NBP would be counterbalanced by a weaker bias in NEE, or vice versa. This would depend mainly on the perturbation of terrestrial NPP and the turnover times of biomass, litter, and

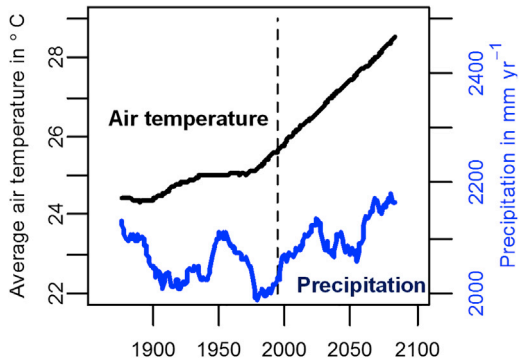

Figure 4. Long-Term Trends of Average Annual Air Temperature (2 m Above Ground) and Precipitation in the Amazon Basin Following IPSL-CM5A-LR Model Outputs under RCP6.0

The graphs represent 30-year running means that suppress interannual variability and reveal temporal trends at the centennial timescale. The dashed vertical line indicates the present day, i.e., the year for which the 30-year running mean corresponds to the average conditions for the period 1981–2010.

soil organic C. Note further that ORCHILEAK represents only the fluvial transfers of DOC and CO_2, and ignores particulate organic carbon (POC). Accordingly, our simulations still underestimate NEE and overestimate NBP. At the present day, POC accounts for only 10% of the total fluvial organic C exports from the Amazon basin.[25] While for the Amazon basin the fluvial export of POC is small compared with that of DOC, global fluvial DOC and POC exports are of a similar magnitude.[44] How far fluvial POC export affects the contemporary NEE and NBP is not trivial to assess and depends on the age of the eroded POC, its degradability, and the rate of SOC replenishment at eroding sites.[45] The quantitative partitioning of the total bias into an NBP overestimate and an NEE underestimate can only be realized with a land-surface model enabled for fluvial C transfers such as ORCHILEAK. The global-scale application of this model is yet to be realized. We have shown that the biases in simulated long-term trends in NEE and NBP scale largely with the temporal evolution of fluvial C exports to the coast. For the Amazon basin, we found that temporal variability in fluvial C exports is strongly controlled by hydrology. If we use the annual values, the correlation is very high ($R^2 = 0.84$), but even when using 30-year running means that suppress interannual variability, the correlation is substantial ($R^2 = 0.38$). At global scale, discharge is projected under RCP6.0 to increase by 7.4% until the end of the 21st century.[46,26] Assuming that DOC exports are generally transport limited, we expect that they will increase at least linearly with discharge. If we weight the projected change in runoff by a spatially explicit estimate of present-day fluvial DOC exports,[47] we estimate an increase in global fluvial DOC exports of 9.6% based on changes in runoff alone.

For the Amazon basin, despite the missing long-term trend in discharge, we simulate an increase in $F_{w\text{-}c,DOC}$ in response to the projected rise in NPP and, thus, litter fall as main DOC source. Increases in terrestrial DOC inputs to inland waters ("browning") have been witnessed in many parts of the globe, and in particular the higher latitudes.[48] In addition, the ongoing permafrost thaw releases increasing amounts of organic C to Arctic rivers.[49] We thus expect that also at global scale, fluvial C exports will increase overproportionally with river discharge over the 21st century. Projections of future trends in fluvial C exports at global scale require a new generation of land-surface models, as represented here with ORCHILEAK, which represent the C cycling along the land-river continuum in response to rising atmospheric CO_2 concentrations, climate change, and LUC. Moreover, we conclude that existing future projections of global NEE and NBP, which were performed by the classical land-surface model, are afflicted by significant biases that increase in magnitude over the simulation period.

EXPERIMENTAL PROCEDURES

Resource Availability

Lead Contact

Further information and requests for resources should be directed to and will be fulfilled by the Lead Contact, Ronny Lauerwald (ronny.lauerwald@gmail.com).

Materials Availability

This study did not generate new unique materials.

Data and Code Availability

The model code used in this study is available at https://doi.org/10.14768/20190423002.1.

Table 2 lists all forcing data used in the simulations. For climate variables, reconstructed historical and projected future data from ISIMIP2 have been used, i.e., model outputs of IPSL ESM following the Representative Concentration Pathway (RCP) 6.0 (cf. Frieler et al.[26]) (see Figure 4). These data are available at https://esg.pik-potsdam.de/search/isimip/. Land cover was taken from the fifth Coupled Model Intercomparison Project (CMIP5) and is available at https://luh.umd.edu/data.shtml.

As in Lauerwald et al.,[11] the bankfull discharge at which floodplain inundation starts was derived as medium discharge running ORCHILEAK over the period 1980–2000 (see Lauerwald et al.[11] for details). Data on soil properties and river network are the same as used in Lauerwald et al.[11] Those data are available from the Lead Contact upon request.

Data of observed discharge used in this study are available from the Global Runoff Data Center (GRDC) at www.bafg.de/GRDC.

Finally, we used simulation results obtained with other models, by other research groups, in the framework of ISIMIP2 to support our findings. These data are available at https://esgf-data.dkrz.de/search/esgf-dkrz/.

Experimental Design

The objectives of this study were to quantify the contribution of fluvial C transfers to the C budget of the Amazon basin and its temporal evolution over the period 1861 to 2100. Moreover, we aimed at quantifying the bias introduced by classical land-surface models, which simulate the land C sink while ignoring these fluvial C transfers. For this, we used the novel land-surface model ORCHILEAK,[11] which simulates the effects of increasing atmospheric CO_2 concentrations, climate change, LUC, and harvest on the budgets of vegetation and soil C pools as classically performed by land-surface models, but which also represents the lateral transfers of C along the river-floodplain network of the Amazon basin. In detail, the novel processes in ORCHILEAK include DOC production from canopy and soils, DOC and CO_2 leaching from soils to streams, and DOC decomposition and CO_2 evasion to the atmosphere during its lateral transport in rivers, as well as exchange with the soil carbon and litter stocks on floodplains and in swamps.

We used this model to simulate the C balance between atmosphere and the Amazon basin (NEE), including vegetation, soils, and the river-floodplain network (see Equation 1). In addition, we simulated the changes in C stocks (biomass, litter, SOC) within the Amazon basin (NBP) over time, based on the NEE, the lateral exports related to harvest of crops and wood and the lateral exports of C through the river-floodplain network to the coast (see Equation 2). We then analyzed how the fluvial C transfers change relative to NEE, NBP, and harvest over time.

To assess the bias introduced by a classical land-surface model ignoring fluvial C transfers, we reran simulations with the fluvial C transfers deactivated while all other processes were simulated as before, including river discharge and floodplain inundation. In this model setup, C inputs from the soil carbon, litter, and vegetation pools to the river network were inhibited, while all C fixed by the vegetation was either respired back to the atmosphere or accumulating in the terrestrial C pools. Simulation results from this "land-only" model were compared with the simulation results from the full ORCHILEAK model, or the "land-river" model, to calculate the biases in simulated NEE and NBP when fluvial C transfers are ignored.

Model Description

The model ORCHILEAK is a new branch of ORCHIDEE,[50] the land-surface scheme of the Institut Pierre Simon Laplace Earth System model. The new features of ORCHILEAK were described validated in detail by Lauerwald et al.[11] The only update of the model code used here concerns the simulation of dissolved CO_2 exports from the soil column via surface runoff (considered here to represent shallow subsurface runoff as well) and drainage. In the original version of ORCHILEAK, the CO_2 concentrations in runoff and drainage were fixed to 2 and 20 mg C L^{-1}, respectively, following observed values (see Lauerwald et al.[11]). Here, we scale those concentrations to heterotrophic soil (Rh_{terr}) and root respiration (Ra_{root}), using simulated values for the period 1991–2000 as reference (4.25 g C m^{-2}, Equation 6). A dimensionless correction factor f_{soil} is calculated accordingly, and multiplied by the basic concentrations of 2 and 20 mg C L^{-1} to obtain the temporally and spatially varying CO_2 export concentrations in surface runoff and drainage, respectively:

$$f_{soil} = \frac{Rh_{terr} + Ra_{root}}{4.25\ g\ C\ m^{-2} d^{-1}}. \quad \text{(Equation 6)}$$

The model performance has been evaluated in detail in Lauerwald et al.[11] Simulated monthly values of fluvial DOC fluxes along the Amazon river and its major tributaries were compared against observed fluxes. Nash-Sutcliffe efficiency (NSE) and root-mean-square error (RMSE) were used to quantify the goodness of fit. At Óbidos, the most downstream gauging station on the Amazon river, simulated DOC fluxes agree well with observations as indicated by an NSE of 0.57 and an RMSE of 23% of the average observed DOC flux at that station. Using time series of observations[30] from six sampling locations across the river network, simulated DOC concentrations compare well with observations (R^2 = 0.45, RMSE = 1.45 mg DOC L^{-1}) showing that ORCHILEAK is able to reproduce observed spatiotemporal patterns in fluvial DOC transport within the Amazon basin. Finally, the simulated seasonality (average monthly fluxes) in aquatic CO_2 emissions from the central Amazon basin compared well with data-driven estimates by Richey et al.[17] (R^2 = 0.85, RMSE = 23%).

Simulations

First, ORCHILEAK is run over 15,000 years of simulation, using land cover and atmospheric CO_2 levels for the year 1861, and looping over the climate forcing from 1861 to 1890. At the end of that model run, biomass and soil carbon pools are close to steady state, with changes of only 0.2% over the last century of simulation. Based on these biomass and soil carbon stocks, historical simulations are run from 1861 to 2005 and, from there following RCP 6.0, future projections until 2099 are run with land cover and atmospheric CO_2 levels updated every year. To test the effect of the explicit representation of the inland water C cycle on the simulated C sink, we ran an alternative simulation with the inland water C cycle deactivated. DOC cycling within the soil column is represented as our standard simulation, but without lateral export to the river network. Similarly, CO_2 produced from autotrophic and heterotrophic respiration, including that of litter and SOC decomposition in inundated soils, is assumed to evade directly and completely to the atmosphere. The representation of all other processes and the use of forcing data are exactly the same between the land-river and the land-only model.

Model Limitations

Note that large uncertainties exist regarding the future CO_2 fertilization effect, and in particular in the tropics, because state-of-the-art land-surface models, including ORCHILEAK, still ignore important limitations of biomass growth due to, e.g., nutrient limitation (in particular phosphorus)[39] and stand competition.[40] Even though the Amazon basin is at present a sink for atmospheric CO_2,[14] the projected increase in terrestrial C stocks until the end of the 21st century is likely an overestimation in absence of nutrient limitation (and of climate induced mortality) in the model. Accordingly, the simulated future increase in riverine DOC concentrations, and thus in fluvial DOC export, is likely overestimated. Consequently, this means that also the increase in biases related to NEE and NBP simulated by the land-only model is overestimated, at least in terms of absolute numbers. Note, however, that a lower increase in NBP due to limited biomass growth would at the same time mean that the relative importance of fluvial C transfers in the C budget of the Amazon basin would decrease less than simulated here. This means that in relative terms, on the contrary the biases in NEE and NBP simulated over the 21st century using a classical land-surface model would be higher than estimated here.

Statistical Analysis

Temporal trends are identified by using 30-year running means, which suppresses the interannual variability. For quantifying changes over the simulation period, we refer to a pre-industrial state, a present-day state, and the state at the end of the 21st century. "Present-day" and "end-of-the-21st century" states are calculated as the averages from the simulation years 1981–2010 and 2070–2099, respectively. The pre-industrial state is calculated from the average of the 30 last years of the 15,000 years of simulation required to reach steady-state biomass and soil C (see above). The average values from these periods are used to quantify historical and future changes in water and C fluxes, temperature, and inundation. For changes in biomass and soil C stocks, we refer instead to the simulated values for the single years of 1861 and 2099, and use the averages from 1981 to 2010 as present-day values.

The bias of the land-only model due to neglecting fluvial C transfers is calculated as difference between the simulation results of the land-only model and the land-river model relative to the results of the land-river model. The net effect of representing fluvial C transfers is equal to the bias, but with the opposite sign.

Treatment of Additional Data Used for Model Evaluation

For the evaluation of simulated fluvial exports of DOC and free dissolved CO_2 to the coast, no direct observed fluxes were available. Fluvial DOC exports are reported for Óbidos,[18] about 900 km upstream from the mouth at Macapá. To scale this value to the outlet of the Amazon basin at Macapá, we make two assumptions: (1) the DOC concentration increases by 10% from Óbidos to Macapá, in agreement with empirical findings;[25] (2) the discharge from the Amazon at Macapá, from where no gauging data are available, can be approximated by summing observed discharge from the Amazon at Óbidos, and from the two main tributaries entering the Amazon between Óbidos and Macapá: Rio Tapajos and Rio Xingu. For this, we used the average observed discharges reported by the GRDC, with 178,451 $m^3\ s^{-1}$ for the Amazon at Óbidos, 10,831 $m^3\ s^{-1}$ for the Rio Tabajos at Jatoba, and 8,144 $m^3\ s^{-1}$ for the Rio Xingu at Altamira. From this, we estimate a discharge of 197,426 $m^3\ s^{-1}$ for the Amazon at Macapá.

For calculating an estimate of fluvial exports of free dissolved CO_2, we used the values of CO_2 partial pressure at two stations at Macapá (North Channel and South Channel) reported for four different seasons in the study by Sawakuchi et al.[31] We used the discharge values reported in that study to calculate a discharge weighted average pCO_2, which we then transformed into a CO_2 concentration of 1.1 mg C L^{-1} assuming a water temperature of 29°C, which is characteristic for the lower part of the Amazon mainstem.[11] We then multiplied that concentration by our estimate of discharge at Macapá.

Finally, we compared our simulated long-term trends in NPP with the simulation results of five land-surface models (ORCHIDEE-DGVM,[51] LPJ-GUESS,[52] LPJmL,[53] VISIT,[54] and CARAIB[55]) in the framework of ISIMIP2, which used the exact same climate forcing data as we did in this study. We overlaid those data with the mask for the Amazon basin used in this study and calculated the past and future changes as described above in the subsection Statistical Analysis.

Assessment of Global-Scale Implications

The change in global runoff over the 21st century was taken from WaterGAP2 model results under the ISIMIP2 protocol following the scenario RCP6.0.[46,26] The change was calculate as difference in average runoff over the periods 1981–2010 versus 2070–2099, consistent with the trend analyses of our model

results (see above). To estimate the impact of changing runoff on fluvial DOC exports, we multiplied the relative rates of change by the global, spatially explicit estimates of DOC yields from GlobalNEWS2.[47] Comparing the results with the original GlobalNEWS2 DOC yields, we estimated the change in global DOC exports assuming that DOC concentrations will not change.

ACKNOWLEDGMENTS

R.L. acknowledges funding from the European Union's Horizon 2020 Research and Innovation program under Marie Sklodowska-Curie grant agreement no. 703813 (C-LEAK project), the Cland Convergence Institute, and ISIpedia. All authors acknowledge funding from the European Union's Horizon 2020 research and innovation program under Marie Sklodowska-Curie grant agreement no. 643052 (ITN C-CASCADES). P.F. and P.R. received funding from the European Union's Horizon 2020 research and innovation program under grant agreements 821003 (4C project) and 776810 (VERIFY project), respectively. For their roles in producing, coordinating, and making available the ISIMIP model output, we acknowledge the modeling groups that provided data for this study (ORCHIDEE-DGVM,[51] LPJ-GUESS,[52] LPJmL,[53] VISIT,[54] CARAIB,[55] WaterGAP2[46]) and the ISIMIP coordination team.

AUTHOR CONTRIBUTIONS

R.L., P.C., and P.R. designed the study. R.L. conducted the experiments and wrote the manuscript. All authors contributed to interpretation and discussion of results and improved the manuscript.

DECLARATION OF INTERESTS

The authors declare no competing interests.

Received: January 13, 2020
Revised: April 28, 2020
Accepted: July 28, 2020
Published: August 21, 2020

REFERENCES

1. Zscheischler, J., Mahecha, M.D., Avitabile, V., Calle, L., Carvalhais, N., Ciais, P., Gans, F., Gruber, N., Hartmann, J., Herold, M., et al. (2017). Reviews and syntheses: an empirical spatiotemporal description of the global surface-atmosphere carbon fluxes: opportunities and data limitations. Biogeosciences *14*, 3685–3703.
2. Drake, T.W., Raymond, P.A., and Spencer, R.G.M. (2017). Terrestrial carbon inputs to inland waters: a current synthesis of estimates and uncertainty. Limnol. Oceanogr. Lett. *3*, 132–142.
3. Resplandy, L., Keeling, R.F., Rödenbeck, C., Stephens, B.B., Khatiwala, S., Rodgers, K.B., Long, M.C., Bopp, L., and Tans, P.P. (2018). Revision of global carbon fluxes based on a reassessment of oceanic and riverine carbon transport. Nat. Geosci. *11*, 504–509.
4. Pan, Y., Birdsey, R.A., Fang, J., Houghton, R., Kauppi, P.E., Kurz, W.A., Phillips, O.L., Shvidenko, A., Lewis, S.L., Canadell, J.G., et al. (2011). A large and persistent carbon sink in the world's forests. Science *333*, 988–993.
5. Regnier, P., Friedlingstein, P., Ciais, P., Mackenzie, F.T., Gruber, N., Janssens, I.a., Laruelle, G.G., Lauerwald, R., Luyssaert, S., Andersson, A.J., et al. (2013). Anthropogenic perturbation of the carbon fluxes from land to ocean. Nat. Geosci. *6*, 597–607.
6. Tang, J., Yurova, A.Y., Schurgers, G., Miller, P.A., Olin, S., Smith, B., Siewert, M.B., Olefeldt, D., Pilesjö, P., and Poska, A. (2018). Drivers of dissolved organic carbon export in a subarctic catchment: importance of microbial decomposition, sorption-desorption, peatland and lateral flow. Sci. Total Environ. *622–623*, 260–274.
7. Camino-Serrano, M., Guenet, B., Luyssaert, S., Ciais, P., Bastrikov, V., De Vos, B., Gielen, B., Gleixner, G., Jornet-Puig, A., Kaiser, K., et al. (2018). ORCHIDEE-SOM: modeling soil organic carbon (SOC) and dissolved organic carbon (DOC) dynamics along vertical soil profiles in Europe. Geosci. Model Dev. *11*, 937–957.
8. Tian, H., Yang, Q., Najjar, R.G., Ren, W., Friedrichs, M.A.M., Hopkinson, C.S., and Pan, S. (2015). Anthropogenic and climatic influences on carbon fluxes from eastern North America to the Atlantic Ocean: a process-based modeling study. J. Geophys. Res. G Biogeosci. *120*, 752–772.
9. Kicklighter, D.W., Hayes, D.J., McClelland, J.W., Peterson, B.J., McGuire, A.D., and Melillo, J.M. (2013). Insights and issues with simulating terrestrial DOC loading of Arctic river networks. Ecol. Appl. *23*, 1817–1836.
10. Nakhavali, M., Friedlingstein, P., Lauerwald, R., Tang, J., Chadburn, S., Camino-Serrano, M., Guenet, B., Harper, A., Walmsley, D., Peichl, M., et al. (2018). Representation of dissolved organic carbon in the JULES land surface model (vn4.4-JULES-DOCM). Geosci. Model. Dev. *11*, 593–609.
11. Lauerwald, R., Regnier, P., Camino-Serrano, M., Guenet, B., Guimberteau, M., Ducharne, A., Polcher, J., and Ciais, P. (2017). ORCHILEAK (revision 3875): a new model branch to simulate carbon transfers along the terrestrial-aquatic continuum of the Amazon basin. Geosci. Model Dev. *10*, 3821–3859.
12. Hastie, A., Lauerwald, R., Ciais, P., and Regnier, P. (2019). Aquatic carbon fluxes dampen the overall variation of net ecosystem productivity in the Amazon basin: an analysis of the interannual variability in the boundless carbon cycle. Glob. Chang. Biol. *25*, 2094–2111.
13. Ahlström, A., Canadell, J.G., Schurgers, G., Wu, M., Berry, J.A., Guan, K., and Jackson, R.B. (2017). Hydrologic resilience and Amazon productivity. Nat. Commun. *8*, https://doi.org/10.1038/s41467-017-00306-z.
14. De Almeida Castanho, A.D., Galbraith, D., Zhang, K., Coe, M.T., Costa, M.H., and Moorcroft, P. (2016). Changing Amazon biomass and the role of atmospheric CO_2 concentration, climate, and land use. Glob. Biogeochem. Cycles *30*, 18–39.
15. Cox, P.M., Pearson, D., Booth, B.B., Friedlingstein, P., Huntingford, C., Jones, C.D., and Luke, C.M. (2013). Sensitivity of tropical carbon to climate change constrained by carbon dioxide variability. Nature *494*, 341–344.
16. Noojipady, P., Morton, C.D., Macedo, N.M., Victoria, C.D., Huang, C., Gibbs, K.H., and Bolfe, L.E. (2017). Forest carbon emissions from cropland expansion in the Brazilian Cerrado biome. Environ. Res. Lett. *12*, https://doi.org/10.1088/1748-9326/aa5986.
17. Richey, J.E., Melack, J.M., Aufdenkampe, A.K., Ballester, V.M., and Hess, L.L. (2002). Outgassing from Amazonian rivers and wetlands as a large tropical source of atmospheric CO_2. Nature *416*, 617–620.
18. Moreira-Turcq, P., Seyler, P., Guyot, J.L., and Etcheber, H. (2003). Exportation of organic carbon from the Amazon River and its main tributaries. Hydrol. Process. *17*, 1329–1344.
19. Abril, G., Martinez, J.-M., Artigas, L.F., Moreira-Turcq, P., Benedetti, M.F., Vidal, L., Meziane, T., Kim, J.-H., Bernardes, M.C., Savoye, N., et al. (2014). Amazon River carbon dioxide outgassing fuelled by wetlands. Nature *505*, 395–398.
20. Le Quéré, C., Andrew, R.M., Friedlingstein, P., Sitch, S., Hauck, J., Pongratz, J., Pickers, P.A., Korsbakken, J.I., Peters, G.P., Canadell, J.G., et al. (2018). Global carbon budget 2018. Earth Syst. Sci. Data *10*, 2141–2194.
21. Abril, G., and Borges, A.V. (2019). Ideas and perspectives: carbon leaks from flooded land: do we need to replumb the inland water active pipe? Biogeosciences *16*, 769–784.
22. Johnson, M.O., Galbraith, D., Gloor, M., De Deurwaerder, H., Guimberteau, M., Rammig, A., Thonicke, K., Verbeeck, H., von Randow, C., Monteagudo, A., et al. (2016). Variation in stem mortality rates determines patterns of above-ground biomass in Amazonian forests: implications for dynamic global vegetation models. Glob. Chang. Biol. *22*, 3996–4013.
23. Zhao, M., Heinsch, F.A., Nemani, R.R., and Running, S.W. (2005). Improvements of the MODIS terrestrial gross and net primary production global data set. Remote Sens. Environ. *95*, 164–176.

24. Ceddia, M.B., Villela, A.L.O., Pinheiro, T.F.M., and Wendroth, O. (2015). Spatial variability of soil carbon stock in the Urucu river basin, Central Amazon-Brazil. Sci. Total Environ. *526*, 58–69.

25. Ward, N.D., Krusche, A.V., Sawakuchi, H.O., Brito, D.C., Cunha, A.C., Moura, J.M.S., da Silva, R., Yager, P.L., Keil, R.G., and Richey, J.E. (2015). The compositional evolution of dissolved and particulate organic matter along the lower Amazon River-Óbidos to the ocean. Mar. Chem. *177 pt 2*, 244–256.

26. Frieler, K., Lange, S., Piontek, F., Reyer, C.P.O., Schewe, J., Warszawski, L., Zhao, F., Chini, L., Denvil, S., Emanuel, K., et al. (2017). Assessing the impacts of 1.5ĝ€°C global warming - simulation protocol of the inter-sectoral impact model Intercomparison project (ISIMIP2b). Geosci. Model Dev. *10*, 4321–4345.

27. Nachtergaele, F., Velthuizen, H.van, Verelst, L., Batjes, N.H., Dijkshoorn, K., van Engelen, V.W.P., Fischer, G., Jones, A., and Montanarela, L. (2010). The Harmonized World Soil Database. In Proceedings of the 19th World Congress of Soil Science, Solutions for a Changing World, R. Gilkes and N. Prakongkep, eds. (International Union of Soil Sciences), pp. 34–37.

28. Guimberteau, M., Drapeau, G., Ronchail, J., Sultan, B., Polcher, J., Martinez, J.-M., Prigent, C., Guyot, J.-L., Cochonneau, G., Espinoza, J.C., et al. (2012). Discharge simulation in the sub-basins of the Amazon using ORCHIDEE forced by new datasets. Hydrol. Earth Syst. Sci. *16*, 911–935.

29. Lauerwald, R., Laruelle, G.G., Hartmann, J., Ciais, P., and Regnier, P.A.G. (2015). Spatial patterns in CO_2 evasion from the global river network. Glob. Biogeochem. Cycles *29*, 534–554.

30. Richey, J.E., Hedges, J.I., Devol, A.H., Quay, P.D., Victoria, R., Martinelli, L., and Forsberg, B.R. (1990). Biogeochemistry of carbon in the Amazon river. Limnol. Oceanogr. *35*, 352–371.

31. Sawakuchi, H.O., Neu, V., Ward, N.D., Barros, M.C., Valerio, A.M., Gagne-Maynard, W., Cunha, A.C., Less, D.F.S., Diniz, J.E.M., Brito, D.C., et al. (2017). Carbon dioxide emissions along the lower Amazon River. Front. Mar. Sci. *4*, https://doi.org/10.3389/fmars.2017.00076.

32. Rasera, M.F.F.L., Krusche, A.V., Richey, J.E., Ballester, M.V.R., and Victória, R.L. (2013). Spatial and temporal variability of pCO_2 and CO_2 efflux in seven Amazonian Rivers. Biogeochemistry *116*, 241–259.

33. Zanchi, F.B., Meesters, A.G.C.A., Waterloo, M.J., Kruijt, B., Kesselmeier, J., Luizão, F.J., and Dolman, A.J. (2014). Soil CO_2 exchange in seven pristine Amazonian rain forest sites in relation to soil temperature. Agric. For. Meteorol. *192–193*, 96–107.

34. Sotta, E.D., Veldkamp, E., Guimarães, B.R., Paixão, R.K., Ruivo, M.L.P., and Almeida, S.S. (2006). Landscape and climatic controls on spatial and temporal variation in soil CO_2 efflux in an Eastern Amazonian Rainforest, Caxiuanã, Brazil. For. Ecol. Manage. *237*, 57–64.

35. Malhi, Y. (2012). The productivity, metabolism and carbon cycle of tropical forest vegetation. J. Ecol. *100*, 65–75.

36. Metcalfe, D.B., Meir, P., Aragão, L.E.O.C., Malhi, Y., da Costa, A.C.L., Braga, A., Gonçalves, P.H.L., de Athaydes, J., de Almeida, S.S., and Williams, M. (2007). Factors controlling spatio-temporal variation in carbon dioxide efflux from surface litter, roots, and soil organic matter at four rain forest sites in the eastern Amazon. J. Geophys. Res. Biogeosci. *112*, G04001.

37. Davidson, E.A., Figueiredo, R.O., Markewitz, D., and Aufdenkampe, A.K. (2010). Dissolved CO_2 in small catchment streams of eastern Amazonia: a minor pathway of terrestrial carbon loss. J. Geophys. Res. G Biogeosci. *115*, G04005.

38. Gloor, M., Gatti, L., Brienen, R., Feldpausch, T.R., Phillips, O.L., Miller, J., Ometto, J.P., Rocha, H., Baker, T., de Jong, B., et al. (2012). The carbon balance of South America: a review of the status, decadal trends and main determinants. Biogeosciences *9*, 5407–5430.

39. Goll, D.S., Vuichard, N., Maignan, F., Jornet-Puig, A., Sardans, J., Violette, A., Peng, S., Sun, Y., Kvakic, M., Guimberteau, M., et al. (2017). A representation of the phosphorus cycle for ORCHIDEE (revision 4520). Geosci. Model Dev. *10*, 3745–3770.

40. Westoby, M. (1984). The self-thinning rule. Adv. Ecol. Res. *14*, 167–225.

41. Bloom, A.A., Exbrayat, J.-F., Van Der Velde, I.R., Feng, L., and Williams, M. (2016). The decadal state of the terrestrial carbon cycle: global retrievals of terrestrial carbon allocation, pools, and residence times. Proc. Natl. Acad. Sci. U S A *113*, 1285–1290.

42. Ludwig, W., Probst, J.L., and Kempe, S. (1996). Predicting the oceanic input of organic carbon by continental erosion. Glob. Biogeochem. Cycles *10*, 23–41.

43. Kondo, M., Patra, P.K., Sitch, S., Friedlingstein, P., Poulter, B., Chevallier, F., Ciais, P., Canadell, J.G., Bastos, A., Lauerwald, R., et al. (2020). State of the science in reconciling top-down and bottom-up approaches for terrestrial CO_2 budget. Glob. Chang. Biol. *26*, 1068–1084.

44. Meybeck, M. (1993). Riverine transport of atmospheric carbon - sources, global typology and budget. Water Air Soil Pollut. *70*, 443–463.

45. Naipal, V., Ciais, P., Wang, Y., Lauerwald, R., Guenet, B., and Van Oost, K. (2018). Global soil organic carbon removal by water erosion under climate change and land use change during 1850-2005. Biogeosciences *15*, 4459–4480.

46. Müller Schmied, H., Adam, L., Eisner, S., Fink, G., Flörke, M., Kim, H., Oki, T., Portmann, F.T., Reinecke, R., Riedel, C., et al. (2016). Variations of global and continental water balance components as impacted by climate forcing uncertainty and human water use. Hydrol. Earth Syst. Sci. *20*, 2877–2898.

47. Mayorga, E., Seitzinger, S.P., Harrison, J.A., Dumont, E., Beusen, A.H.W., Bouwman, A.F., Fekete, B.M., Kroeze, C., and Van Drecht, G. (2010). Global nutrient export from WaterSheds 2 (NEWS 2): model development and implementation. Environ. Model. Softw. *25*, 837–853.

48. Lapierre, J.-F., Guillemette, F., Berggren, M., and Del Giorgio, P.A. (2013). Increases in terrestrially derived carbon stimulate organic carbon processing and CO_2 emissions in boreal aquatic ecosystems. Nat. Commun. *4*, 2972.

49. Vonk, J.E., Tank, S.E., Bowden, W.B., Laurion, I., Vincent, W.F., Alekseychik, P., Amyot, M., Billet, M.F., Canário, J., Cory, R.M., et al. (2015). Reviews and syntheses: effects of permafrost thaw on Arctic aquatic ecosystems. Biogeosciences *12*, 7129–7167.

50. Krinner, G., Viovy, N., de Noblet-Ducoudré, N., Ogée, J., Polcher, J., Friedlingstein, P., Ciais, P., Sitch, S., and Prentice, I.C. (2005). A dynamic global vegetation model for studies of the coupled atmosphere-biosphere system. Glob. Biogeochem. Cycles *19*, https://doi.org/10.1029/2003GB002199.

51. Guimberteau, M., Zhu, D., Maignan, F., Huang, Y., Yue, C., Dantec-Nédélec, S., Ottlé, C., Jornet-Puig, A., Bastos, A., Laurent, P., et al. (2018). ORCHIDEE-MICT (v8.4.1), a land surface model for the high latitudes: model description and validation. Geosci. Model Dev. *11*, 121–163.

52. Smith, B., Wårlind, D., Arneth, A., Hickler, T., Leadley, P., Siltberg, J., and Zaehle, S. (2014). Implications of incorporating N cycling and N limitations on primary production in an individual-based dynamic vegetation model. Biogeosciences *11*, 2027–2054.

53. Bondeau, A., Smith, P.C., Zaehle, S., Schaphoff, S., Lucht, W., Cramer, W., Gerten, D., Lotze-campen, H., Müller, C., Reichstein, M., et al. (2007). Modelling the role of agriculture for the 20th century global terrestrial carbon balance. Glob. Chang. Biol. *13*, 679–706.

54. Ito, A., and Oikawa, T. (2002). A simulation model of the carbon cycle in land ecosystems (Sim-CYCLE): a description based on dry-matter production theory and plot-scale validation. Ecol. Modell. *151*, 143–176.

55. Warnant, P., François, L., Strivay, D., and Gérard, J.-C. (1994). CARAIB: a global model of terrestrial biological productivity. Glob. Biogeochem. Cycles *8*, 255–270.